axioms

MDPI

Article

Scale Mixture of Akash Distribution with Applications to Income Data

Neveka M. Olmos [1], Luis Firinguetti-Limone [2], Diego I. Gallardo [2], Osvaldo Venegas [3,*] and Héctor W. Gómez [1]

[1] Departamento de Estadística y Ciencias de Datos, Facultad de Ciencias Básicas, Universidad de Antofagasta, Antofagasta 1240000, Chile; neveka.olmos@uantof.cl (N.M.O.); hector.gomez@uantof.cl (H.W.G.)
[2] Departamento de Estadística, Facultad de Ciencias, Universidad del Bío-Bío, Concepción 4081112, Chile; lfiringu@ubiobio.cl (L.F.-L.); dgallardo@ubiobio.cl (D.I.G.)
[3] Departamento de Ciencias Matemáticas y Físicas, Facultad de Ingeniería, Universidad Católica de Temuco, Temuco 4780000, Chile
* Correspondence: ovenegas@uct.cl

Abstract

In this paper, the scale mixture of Akash (SMAK) distribution is introduced. This new distribution results from a scale mixture of the Akash distribution and the exponential distribution. The SMAK distribution is an alternative to two-parameter distributions with a heavy right tail. We study its representation, some basic properties, and maximum likelihood inference. We carry out three applications with real data, in which the SMAK distribution exhibits better performance than other distributions.

Keywords: Akash distribution; heavy-tailed distribution; maximum likelihood

MSC: 62E15; 62F12; 62P05

1. Introduction

The slash distribution is an extension of the normal distribution, based on a quotient of two independent random variables: one normally distributed and the other a power of the uniform distribution. A random variable Y is said to have a slash distribution if it can be expressed as

$$Y = ZU^{-1/q}, \tag{1}$$

where $Z \sim N(0,1)$, $U \sim \text{Uniform}(0,1)$, Z and U are independent, and $q > 0$ (see Johnson et al. [1]). This distribution has heavier tails than the normal distribution. Rogers and Tukey [2] and Mosteller and Tukey [3] discuss its properties. Kadafar [4] discuss maximum likelihood (ML) estimators of location and scale. Wang and Genton [5] provide a multivariate version of the slash distribution, as well as a multivariate skew version. Gómez et al. [6] and Gómez et al. [6] extend the slash distribution using the family of univariate and multivariate elliptical distributions. This methodology to increase tail weight has also been used in distributions with positive support, for example, Olmos et al. [7] in the generalized half-normal distributions, Astorga et al. [8] in the power Muth distribution, and Gómez et al. [9] in the Akash distribution, among others. All slash distributions are a particular case of the scale mixture family (see Andrews and Mallows [10]). In particular, Gómez et al. [9] introduced a slash extension of the Akash distribution by considering a Beta mixing variable. The resulting model provides greater flexibility than the original Akash distribution, particularly in terms of its kurtosis and tail behavior. Although the

Check for updates

Academic Editor: Tao Liu

Received: 10 July 2026
Revised: 18 August 2026
Accepted: 28 August 2026
Published: 2 September 2026

Copyright: © 2026 by the authors. Licensee MDPI, Basel, Switzerland. This article is an open access article distributed under the terms and conditions of the Creative Commons Attribution (CC BY) license.

present work is also based on a scale mixture construction of the Akash distribution, our approach differs from that of Gómez et al. [9] in both the choice of the mixing distribution and the resulting tail properties. Specifically, we consider an exponential mixing distribution, which leads to a different stochastic representation and, as shown below, to an extremely heavy right tail. Shanker [11] introduces the Akash (AK) distribution and applies it to real lifetime datasets from medical science and engineering. Thus, we say that a random variable Y has the AK distribution with scale parameter σ, and shape parameter θ if its probability density function (PDF) is given by

$$f_Y(y;\sigma,\theta) = \frac{\theta^3}{\sigma(\theta^2+2)}\left(1+\frac{y^2}{\sigma^2}\right)\exp\left(-\frac{\theta y}{\sigma}\right), \quad y>0, \tag{2}$$

where $\sigma > 0$ is a scale parameter and $\theta > 0$ is a shape parameter, we denote it by $Y \sim AK(\sigma,\theta)$. Some properties of the AK distribution are

1. $\mathbb{E}(Y) = \dfrac{\sigma(\theta^2+6)}{\theta(\theta^2+2)}$; $Var(Y) = \dfrac{\sigma^2(\theta^4+16\theta^2+12)}{\theta^2(\theta^2+2)^2}$.
2. $\mathbb{E}(Y^r) = \dfrac{r!\sigma^r(\theta^2+(r+1)(r+2))}{\theta^r(\theta^2+2)}$, for $r = 1,2,\ldots$
3. $M_Y(t) = \dfrac{\theta^3}{\theta^2+2}\left(\dfrac{(\theta-\sigma t)^2+2}{(\theta-\sigma t)^3}\right)$, for $t < \theta/\sigma$

Extensions of the AK distribution have been made by Shanker and Shukla [12,13] and Gómez et al. [9], among others.

From item 3, we note that the moment-generating function of the AK distribution is finite for all $t < \theta/\sigma$, indicating that the AK distribution is not heavy-tailed (see Foss et al. [14]); namely, the AK distribution does not have sufficient flexibility to model datasets containing outliers. Therefore, the main objective of this article is to study the scale mixture of Akash (SMAK) distribution, which features a simple expression and offers greater flexibility for modeling positive data with a heavy right tail. The SMAK distribution can serve as an alternative to the log-normal distribution (see Aitchison and Brown [15]), commonly used to model income data (see Kleiber and Kotz [16]).

The article is developed as follows. In Section 2 we present the SMAK distribution and its properties. In Section 3 we perform parameter estimation using the ML method via the EM algorithm, in addition to presenting a simulation study and the asymptotic convergence of the ML estimators. In Section 4 we perform three applications with real data. In Section 5 we provide some concluding remarks.

2. New Density and Its Properties

In this section, we introduce the PDF and the properties of the SMAK distribution.

2.1. Density Function

Definition 1. *We say that $X \sim SMAK(\lambda,\theta)$. Then, the PDF of X is given by*

$$f_X(x;\lambda,\theta) = \frac{\lambda\theta^3}{\theta^2+2}\left\{\frac{(\theta x+\lambda)^2+6x^2}{(\theta x+\lambda)^4}\right\}, \quad x>0, \tag{3}$$

where $\lambda > 0$ is a scale parameter and $\theta > 0$ is a shape parameter.

Table 1 shows $P(X > x)$ for different values of x for the mentioned distribution. Figure 1 shows the graphs of the SMAK distribution for different values of the parameter θ. We observe that as θ decreases, the SMAK distribution exhibits a heavier tail.

Table 1. Tails comparison.

Distribution	$P(X > 4)$	$P(X > 6)$	Distribution	$P(X > 10)$	$P(X > 15)$
SMAK(1,2)	0.173	0.122	SMAK(1,0.2)	0.696	0.572
SMAK(1,4)	0.071	0.048	SMAK(1,0.4)	0.467	0.353
SMAK(1,6)	0.044	0.030	SMAK(1,0.6)	0.336	0.245

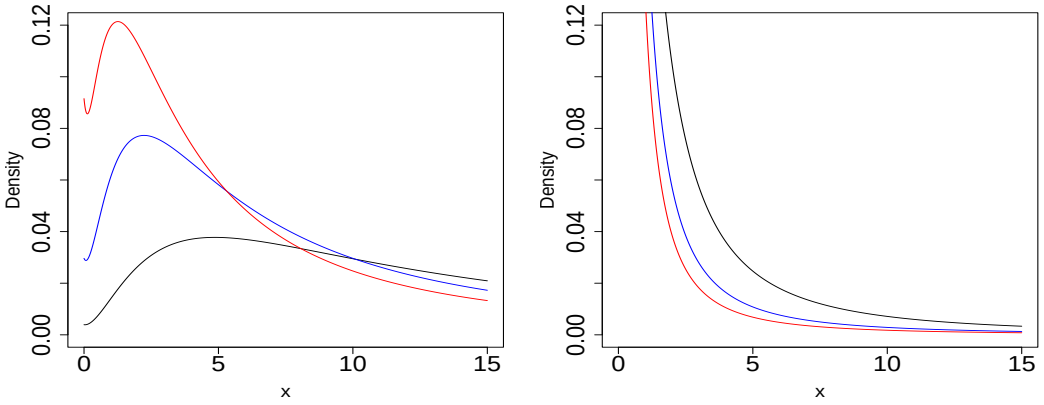


Figure 1. (**Left**) panel: Plots of PDFs of SMAK(1, 0.2) (black), SMAK(1, 0.4) (blue), and SMAK(1, 0.6) (red). (**Right**) panel: Plots of PDFs of SMAK(1, 2) (black), SMAK(1, 4) (blue), and SMAK(1, 6) (red).

2.2. Properties

The following proposition shows that the PDF of the SMAK distribution can be represented as a scale mixture of the AK and exponential (Exp) distributions.

Proposition 1. *If* $X|U = u \sim AK(u^{-1}, \theta)$ *and* $U \sim Exp(\lambda)$, *then* $X \sim SMAK(\lambda, \theta)$.

Proof. By directly computing the integral, we have

$$f_X(x;\lambda,\theta) = \int_{Rec(u)} f_{X|U}(x) f_U(u) du = \frac{\lambda\theta^3}{\theta^2+2} \int_0^\infty (u + x^2u^3) \exp(-(\theta x + \lambda)u) du,$$

the result is obtained by applying the change of variable $t = (\theta x + \lambda)u$. □

Proposition 2. *Let* $Y \sim AK(1, \theta)$ *and* $U \sim Exp(\lambda)$ *be independent random variables. Then* $X = YU^{-1} \sim SMAK(\lambda, \theta)$.

Proof. Using the Jacobian method, we have

$$\left.\begin{array}{l} X = YU^{-1} \\ V = U \end{array}\right\} \Rightarrow \left.\begin{array}{l} Y = XV \\ U = V \end{array}\right\} \Rightarrow J = \begin{vmatrix} \frac{\partial y}{\partial x} & \frac{\partial y}{\partial v} \\ \frac{\partial u}{\partial x} & \frac{\partial u}{\partial v} \end{vmatrix} = \begin{vmatrix} v & x \\ 0 & 1 \end{vmatrix} = v.$$

$$\begin{aligned} f_{X,V}(x,v) &= |J| f_{Y,U}(xv, v). \\ f_{X,V}(x,v) &= v f_Y(xv) f_U(v). \\ f_{X,V}(x,v) &= \frac{v\theta^3}{\theta^2+2}(1 + x^2v^2) \exp(-\theta xv)\lambda \exp(-\lambda v)\,,\ x > 0\,,\ v > 0. \end{aligned}$$

Then, marginalizing with respect to V, we obtain the density function associated with X:

$$f_X(x;\lambda,\theta) = \frac{\lambda\theta^3}{\theta^2+2} \int_0^\infty (v + x^2v^3) \exp(-\theta xv)\lambda \exp(-\lambda v), \quad x > 0, \quad v > 0.$$

Making the change of variable $t = (\theta x + \lambda)v$, the result is obtained. □

Two algorithms can be used to generate random numbers from the SMAK distribution, as shown below. Algorithm 1 uses Proposition 1 and the composition method (see Tanner [17]). Algorithm 2 uses the representation given in Proposition 2.

Algorithm 1 for simulating from the $X \sim SMAK(\lambda, \theta)$ can proceed as follows

1: Generate $U \sim Exp(\lambda)$.
2: Compute $X|U = u \sim AK(u^{-1}, \theta)$.

Algorithm 2 for simulating from the $X \sim SMAK(\lambda, \theta)$ can proceed as follows

1: Generate $S \sim Exp(\theta)$
2: Generate $T \sim Gamma(3, \theta)$
3: Generate $V \sim Bernoulli\left(\frac{\theta}{1+\theta}\right)$
4: Compute $Y = VS + (1 - V)T$
5: Generate $U \sim Exp(\lambda)$
6: Compute $X = \frac{Y}{U}$

Proposition 3. *Let $X \sim SMAK(\lambda, \theta)$. Then*

1. *The density function $f_X(x)$ is strictly decreasing whenever $\theta > \frac{\sqrt{3}}{2}$.*
2. *If $\theta \leq \frac{\sqrt{3}}{2}$, the anti-mode and the mode of the SMAK distribution are given, respectively, by*

$$\lambda\left(\frac{3 - \theta^2 - \sqrt{9 - 12\theta^2}}{\theta(6 + \theta^2)}\right) \quad \text{and} \quad \lambda\left(\frac{3 - \theta^2 + \sqrt{9 - 12\theta^2}}{\theta(6 + \theta^2)}\right).$$

Proof. By differentiating the PDF in (3) with respect to x, we obtain

$$f'_X(x) = \frac{2\lambda\theta^3}{\theta^2 + 2} \cdot \frac{-(\theta^2 + 6)\theta x^2 + 2\lambda(3 - \theta^2)x - \theta\lambda^2}{(\theta x + \lambda)^5}.$$

Observe that the sign and the zeros of $f'_X(x)$ are completely determined by the quadratic polynomial

$$g(x) = -(\theta^2 + 6)\theta x^2 + 2\lambda(3 - \theta^2)x - \theta\lambda^2.$$

Since the leading coefficient of $g(x)$ is $-(\theta^2 + 6)\theta < 0$ and its discriminant is $\Delta = 12\lambda^2(3 - 4\theta^2)$, it follows that $\Delta < 0$ whenever $\theta > \frac{\sqrt{3}}{2}$. Under this condition, $g(x) < 0$ for all x, and hence $f'_X(x) < 0$, which proves the first result. The second result follows directly from solving $g(x) = 0$. □

The following proposition shows the cumulative distribution function (CDF) of the SMAK distribution.

Proposition 4. *Let $X \sim SMAK(\lambda, \theta)$. Then the CDF of X is given by*

$$F_X(x; \lambda, \theta) = \frac{\theta^3 x[(2 + \theta^2)x^2 + 2\lambda\theta x + \lambda^2]}{(\theta^2 + 2)(\theta x + \lambda)^3}, \quad x > 0, \tag{4}$$

where $\lambda, \theta > 0$.

Proof. By directly computing the CDF of X we have

$$F_X(x; \lambda, \theta) = \int_0^x \frac{\lambda\theta^3}{\theta^2 + 2}\left\{\frac{(\theta t + \lambda)^2 + 6t^2}{(\theta t + \lambda)^4}\right\}dt;$$

then, applying the change of variable $u = \theta t + \lambda$, the result is obtained. □

2.3. Reliability Analysis

The reliability function $r(t)$ and the hazard function $h(t)$ of the SMAK distribution are given in the following corollary.

Corollary 1. *Let $T \sim SMAK(\lambda, \theta)$. Then $r(t)$ and $h(t)$ of T are given by*

$$r(t) = \frac{\lambda[\theta^2(\theta^2+6)t^2 + 2\lambda\theta(\theta^2+3)t + (\theta^2+2)\lambda^2]}{(\theta^2+2)(\theta t+\lambda)^3},$$

$$h(t) = \frac{\theta^3[(\theta t+\lambda)^2 + 6t^2]}{(\theta t+\lambda)[\theta^2(\theta^2+6)t^2 + 2\lambda\theta(\theta^2+3)t + (\theta^2+2)\lambda^2]},$$

where $\lambda, \theta, t > 0$.

In Figure 2, we show the hazard function of the SMAK distribution for several values of θ.

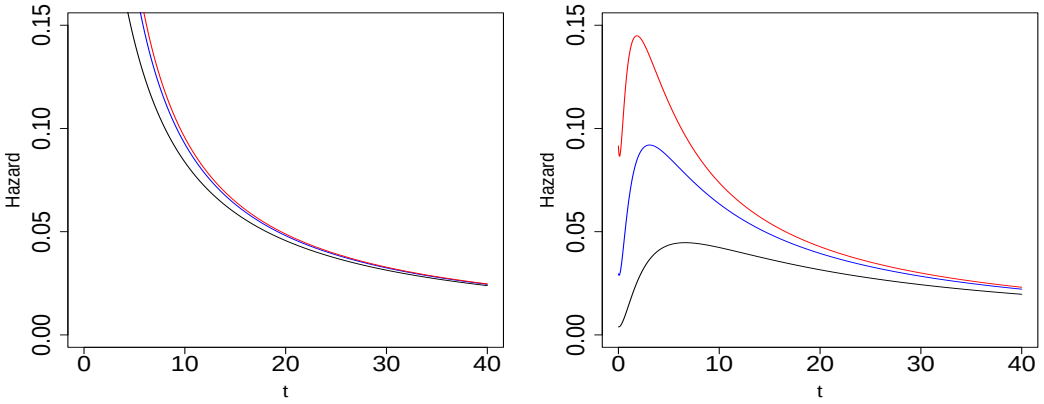


Figure 2. (**Left**) panel: Plots of hazard functions of SMAK(1, 1) (black), SMAK(1, 2) (blue), and SMAK(1, 3) (red). (**Right**) panel: Plots of hazard functions of SMAK(1, 0.2) (black), SMAK(1, 0.4) (blue), and SMAK(1, 0.6) (red).

Remark 1.

1. *We note that for $t \to \infty$, $h(t) \sim 1/t$, which implies that $h(t) = O(1/t)$. Moreover, for $t \to 0$, $h(t) \to \frac{\theta^3}{\lambda(\theta^2+2)}$.*
2. *The hazard function for some parameter values exhibits a decreasing behavior, while for other values it will have a unimodal or inverted bathtub shape.*

The following lemma is necessary for the proposition below.

Lemma 1. *For $\lambda > 0$ and $r = 1, 2, \ldots$, it holds that*

$$\int_0^1 \frac{\exp(-\lambda t)}{t^r} dt = \infty.$$

Proof. For $t \in (0, 1]$, we have $\exp(-\lambda t) \geq \exp(-\lambda) > 0$. Using this inequality, we obtain

$$\int_0^1 \frac{\exp(-\lambda t)}{t^r} dt \geq \exp(-\lambda) \int_0^1 \frac{1}{t^r} dt,$$

and the result follows since the integral on the right-hand side diverges for $r = 1, 2, \ldots$ □

Proposition 5. *The r-th moments of the random variable $X \sim SMAK(\lambda, \theta)$ do not exist, with $r = 1, 2, 3, \ldots$.*

Proof. Using Proposition 1, we have

$$\mathbb{E}(X^r) = \mathbb{E}(\mathbb{E}(X^r|U)) = \mathbb{E}\left(\frac{r!U^{-r}(\theta^2 + (r+1)(r+2))}{\theta^r(\theta^2+2)}\right) = \left(\frac{r!(\theta^2 + (r+1)(r+2))}{\theta^r(\theta^2+2)}\right)\mathbb{E}(U^{-r}),$$

where $\mathbb{E}(U^{-r}) = \int_0^\infty u^{-r}\lambda\exp(-\lambda u)du = \lambda\int_0^1 u^{-r}\exp(-\lambda u)du + \lambda\int_1^\infty u^{-r}\exp(-\lambda u)du$, the result follows by directly applying Lemma 1 to the first integral on the right-hand side. □

Remark 2. *Proposition 5 shows that the SMAK distribution does not possess finite positive moments. This implies that the mean and variance are not finite, which has important practical implications. First, use the distribution for data with extremely heavy tails, where traditional moment-based summary statistics are unreliable. In such settings, robust measures such as the median and quantiles are recommended for describing the data. Second, parameter interpretation should focus on their influence on the hazard function and tail behavior rather than on moment-based quantities. Third, likelihood-based inference remains valid, and model comparison can be safely performed using AIC and BIC. Finally, the SMAK distribution is comparable to other heavy-tailed models (e.g., certain Pareto or stable distributions) that also lack finite moments, and its use is justified when the data exhibit extreme observations.*

2.4. Order Statistics

Let $X_1, \ldots, X_n$ be a random sample from the random variable $X \sim SMAK(\lambda, \theta)$, let us denote by $X_{(j)}$ the *jth* - order statistics, $j \in \{1, \ldots, n\}$.

Proposition 6. *The PDF of $X_{(j)}$ is*

$$\begin{aligned} f_{X_{(j)}}(x) &= \frac{n!\lambda\theta^3}{(j-1)!(n-j)!(\theta^2+2)^n}\left\{\frac{(\theta x+\lambda)^2+6x^2}{(\theta x+\lambda)^{3n+1}}\right\}\left\{\theta^3 x\left[(2+\theta^2)x^2+2\lambda\theta x+\lambda^2\right]\right\}^{j-1} \\ &\times \left\{\lambda\left[\theta^2(\theta^2+6)x^2+2\lambda\theta(\theta^2+3)x+(\theta^2+2)\lambda^2\right]\right\}^{n-j}, \quad x>0. \end{aligned}$$

In particular, the PDF of the minimum, $X_{(1)}$, is

$$f_{X_{(1)}}(x) = \frac{n\lambda\theta^3}{(\theta^2+2)^n}\left\{\frac{(\theta x+\lambda)^2+6x^2}{(\theta x+\lambda)^{3n+1}}\right\}\left\{\lambda\left[\theta^2(\theta^2+6)x^2+2\lambda\theta(\theta^2+3)x+(\theta^2+2)\lambda^2\right]\right\}^{n-1}, \quad x>0$$

and the PDF of the maximum, $X_{(n)}$, is

$$f_{X_{(n)}}(x) = \frac{n\lambda\theta^3}{(\theta^2+2)^n}\left\{\frac{(\theta x+\lambda)^2+6x^2}{(\theta x+\lambda)^{3n+1}}\right\}\left\{\theta^3 x\left[(2+\theta^2)x^2+2\lambda\theta x+\lambda^2\right]\right\}^{n-1}, \quad x>0.$$

Proof. Since we are dealing with an absolutely continuous model, the PDF of the *j*th-order statistics is obtained by applying

$$f_{X_{(j)}}(x) = \frac{n!}{(j-1)!(n-j)!}f(x)[F(x)]^{j-1}[1-F(x)]^{n-j}, \quad j \in \{1, \ldots, n\}$$

where F and f denote the CDF and PDF of the parent distribution, $X \sim SMAK(\lambda, \theta)$ in this case. □

RightTail of the SMAK Distribution

Heavy-tailed distributions are very important in economics and finance. For positive data, heavy-tailed distributions are those whose right-tail probabilities are greater than those of the exponential distribution (see Beirlant et al. [18] and Foss et al. [14]). In other words, a non-negative function is heavy-tailed if it is not bounded by the exponential distribution. More precisely, the definition states the following:

Definition 2. *A function $f \geq 0$ is said to be heavy-tailed if and only if*

$$\lim_{x\to\infty} \sup e^{\alpha x} f(x) = \infty, \quad \alpha > 0.$$

Proposition 7. *Let $X \sim SMAK(\lambda, \theta)$. Then, the SMAK distribution has a heavy tail.*

Proof. By applying L'Hôpital's Rule four times, we have

$$\begin{aligned}
\lim_{x\to\infty} \sup e^{\alpha x} f_X(x;\lambda,\theta) &= \lim_{x\to\infty} \sup \frac{\lambda\theta^3 e^{\alpha x}\{(\theta x+\lambda)^2+6x^2\}}{(\theta^2+2)(\theta x+\lambda)^4} \\
&= \lim_{x\to\infty} \sup \frac{\lambda\theta^3\alpha^2 e^{\alpha x}\{\alpha^2 u(x)+8\alpha\theta(\theta x+\alpha)+48\alpha x+12\theta^2+72\}}{24\theta^4(\theta^2+2)} \\
&= \infty,
\end{aligned}$$

where $u(x) = (\theta x + \lambda)^2 + 6x^2$. □

Some works with heavy-tailed distributions that have been used in actuarial statistics are as follows: Zhao et al. [19] presents a new family of heavy-tailed distributions, useful for modeling financial data; Riad et al. [20] in the new Kayva–Manoharan–Lomaxmodel, with a real data application related to HT insurance loss; Afify et al. [21] in the exponential-power-weighted model to model financial data, among other heavy tail model.

3. Inference

In this section, we estimate the SMAK parameters using the ML method via the expectation–maximization (EM) algorithm. Other estimation approaches could also be considered for the SMAK model, including moment-based methods, minimum distance or discrepancy-based procedures, and Bayesian estimation. However, the use of moment-based methods is not particularly attractive in the present setting because, as established in Proposition 5, the SMAK distribution does not possess positive moments. This prevents the direct use of conventional moment-based estimation procedures based on theoretical moments. Distance-based methods remain possible, but their implementation requires the selection of an appropriate distance or weighting scheme. Bayesian estimation would additionally require the specification of prior distributions for the model parameters. In contrast, ML provides a natural and fully parametric estimation framework based directly on the distributional form of the SMAK model, without requiring such additional choices. Moreover, the likelihood can be evaluated explicitly through the stochastic representation developed in Section 2, which makes ML estimation particularly convenient for the proposed model.

3.1. ML Estimation

Let $X_1, \ldots, X_n$ be a random sample with n terms distributed $X \sim SMAK(\lambda, \theta)$, then the log-likelihood function for $\boldsymbol{\eta} = (\lambda, \theta)$ can be expressed as

$$\ell(\boldsymbol{\eta}) = 3n\log(\theta) + n\log(\lambda) - n\log(2+\theta^2) + \sum_{i=1}^{n}\log\left((\theta x_i+\lambda)^2+6x_i^2\right) - 4\sum_{i=1}^{n}\log(\theta x_i+\lambda), \tag{5}$$

Taking partial derivatives in $\ell(\boldsymbol{\eta})$ with respect to λ and θ and setting them equal to zero, we obtain

$$\sum_{i=1}^{n} \frac{\theta x_i + \lambda}{(\theta x_i + \lambda)^2 + 6x_i^2} - \sum_{i=1}^{n} \frac{2}{\theta x_i + \lambda} = -\frac{n}{2\lambda},$$

$$\sum_{i=1}^{n} \frac{x_i(\theta x_i + \lambda)}{(\theta x_i + \lambda)^2 + 6x_i^2} - \sum_{i=1}^{n} \frac{2x_i}{\theta x_i + \lambda} = \frac{n\theta}{2+\theta^2} - \frac{3n}{2\theta},$$

Solving this system of equations numerically to find the ML estimates may not be so simple; in this case, an EM algorithm can be implemented (see Dempster et al. [22]) to obtain these ML estimates. The following subsection is dedicated to this objective.

3.2. EM Algorithm

Using Proposition 1, the SMAK distribution admits the hierarchical representation $U_i \sim \text{Exp}(\lambda)$, and $X_i|U_i = u_i \sim AK(u_i^{-1}, \theta)$. Therefore, for a random sample $x_1, \ldots, x_n$, the complete log-likelihood function is

$$\ell_c(\boldsymbol{\eta}) = n\log\lambda + 3n\log\theta - n\log(\theta^2+2) + \sum_{i=1}^{n}\log u_i + \sum_{i=1}^{n}\log(1+x_i^2u_i^2) - \theta\sum_{i=1}^{n}x_iu_i - \lambda\sum_{i=1}^{n}u_i. \tag{6}$$

Note that the E-step only requires the computation of the expectation for $U_i|X_i = x_i$. The conditional density of $U_i|X_i = x_i$ is

$$f(u_i|x_i) \propto (u_i + u_i^3x_i^2)e^{-a_iu_i} = u_ie^{-a_iu_i} + x_i^2u_i^3e^{-a_iu_i},$$

where $a_i = \theta x_i + \lambda$. Therefore, $U_i|x_i \sim p_i\,\Gamma(2, a_i) + (1-p_i)\,\Gamma(4, a_i)$, with $p_i = a_i^2/(a_i^2 + 6x_i^2)$, i.e., a mixture of two gammas. Therefore, it is immediate that

$$\mathbb{E}(U_i|X_i = x_i) = \frac{2p_i + 4(1-p_i)}{a_i}. \tag{7}$$

Therefore, the Q-function is expressed as $Q(\boldsymbol{\eta}) = \mathbb{E}\left[\ell_c(\boldsymbol{\eta}) \mid \mathbf{x}, \lambda^{(t)}, \theta^{(t)}\right]$. Ignoring terms that do not depend on λ and θ, we obtain

$$Q(\boldsymbol{\eta}) = n\log\lambda + 3n\log\theta - n\log(\theta^2+2) - \theta\sum_{i=1}^{n}x_im_i^{(t)} - \lambda\sum_{i=1}^{n}m_i^{(t)}, \tag{8}$$

where $m_i^{(t)} = \mathbb{E}(U_i \mid X_i = x_i, \theta = \theta^{(t)}, \lambda = \lambda^{(t)})$. The maximization required for the M-step yields a closed-form solution for λ, but requires solving a non-linear equation for θ. In summary, the EM algorithm is given by the steps in Algorithm 3.

Algorithm 3 EM algorithm for SMAK distribution.

1: Choose initial values $(\lambda^{(0)}, \theta^{(0)})$.
2: For $t = 0, 1, \ldots$

E-step. Compute $a_i^{(t)} = \theta^{(t)}x_i + \lambda^{(t)}$, $p_i^{(t)} = \dfrac{\left(a_i^{(t)}\right)^2}{\left(a_i^{(t)}\right)^2 + 6x_i^2}$, and $m_i^{(t)} = \dfrac{4-2p_i^{(t)}}{a_i^{(t)}}$.

M-step. Update λ as $\lambda^{(t+1)} = \dfrac{n}{\sum_{i=1}^{n} m_i^{(t)}}$.

Compute $A^{(t)} = \sum_{i=1}^{n} x_im_i^{(t)}$, and obtain $\theta^{(t+1)}$ as the solution of

$$A^{(t)}\theta^3 - n\theta^2 + 2A^{(t)}\theta - 6n = 0.$$

The algorithm stops when a suitable rule is satisfied. For instance, $|\ell^{(t+1)} - \ell^{(t)}| < \varepsilon$. On the other hand, the covariance matrix of the ML estimators is estimated from the inverse of the observed information matrix. Specifically, letting $\widehat{\boldsymbol{\eta}} = (\widehat{\lambda}, \widehat{\theta})^\top$ as the estimators obtained at the convergence, we have

$$\widehat{\mathrm{Var}}(\widehat{\boldsymbol{\eta}}) = -\left[\frac{\partial^2 \ell(\boldsymbol{\eta})}{\partial \boldsymbol{\eta} \partial \boldsymbol{\eta}^\top}\right]^{-1}_{\boldsymbol{\eta}=\widehat{\boldsymbol{\eta}}}. \tag{9}$$

Consequently, the standard error of $\widehat{\eta}_j$ is obtained as

$$\mathrm{SE}(\widehat{\eta}_j) = \sqrt{\left[\widehat{\mathrm{Var}}(\widehat{\boldsymbol{\eta}})\right]_{jj}}, \qquad j = 1, 2. \tag{10}$$

3.3. Simulation Study

To examine the behavior of the ML estimation, we conducted a simulation study to evaluate its performance in estimating the parameters λ and θ of the SMAK model. For each simulation scenario, random samples from the SMAK(λ, θ) distribution were generated using Algorithm 2 described in Section 2.2. Specifically, for each observation, we generated $S_i \sim \mathrm{Exp}(\theta)$, $T_i \sim \mathrm{Gamma}(3, \theta)$, and $V_i \sim \mathrm{Bernoulli}(\theta/(1+\theta))$, and defined $Y_i = V_i S_i + (1 - V_i) T_i$. Independently, we generated $U_i \sim \mathrm{Exp}(\lambda)$ and then obtained the simulated observation as $X_i = Y_i / U_i$. Thus, the simulation procedure follows directly from the stochastic representation given in Proposition 2. The simulation analysis was carried out by generating 1000 replicates of sizes $n = 50$, 100, 200, and 500 from the SMAK model, resulting in 36 simulation scenarios and a total of 36,000 simulated samples. For each generated sample, the ML estimates were obtained using the EM algorithm. Table 2 presents the empirical bias (Bias), the mean of the estimated standard errors (SE), and the root mean square error (RMSE). For each replication, the standard errors were obtained from the estimated covariance matrix of the ML estimators. For each simulation scenario, the SE reported in Table 2 corresponds to the average of the estimated standard errors over the 1000 replications.

Table 2. Bias, SE and RMSE of $\hat{\lambda}$ and $\hat{\theta}$ in the SMAK model.

True Values		EstiMator	$n = 50$			$n = 100$			$n = 200$			$n = 500$		
λ	θ		Bias	SE	RMSE	Bias	SE	RMSE	Bias	SE	RMSE	Bias	SE	RMSE
0.25	0.25	$\widehat{\lambda}$	−0.148	0.576	0.564	−0.088	0.349	0.302	−0.018	0.221	0.186	−0.007	0.133	0.121
		$\widehat{\theta}$	−0.152	0.421	0.293	−0.082	0.291	0.203	−0.016	0.199	0.158	−0.007	0.123	0.110
	1	$\widehat{\lambda}$	−0.006	1.030	0.828	−0.016	0.689	0.735	−0.007	0.374	0.555	−0.001	0.150	0.349
		$\widehat{\theta}$	−0.004	1.565	1.192	−0.040	1.092	1.077	−0.023	0.630	0.811	−0.003	0.288	0.516
	2	$\widehat{\lambda}$	0.132	1.139	0.476	0.117	0.939	0.455	0.112	0.707	0.412	0.117	0.523	0.390
		$\widehat{\theta}$	0.574	5.213	2.052	0.522	4.298	2.038	0.512	3.229	1.858	0.554	2.358	1.734
1	0.25	$\widehat{\lambda}$	−0.560	2.049	1.499	−0.327	1.354	1.061	−0.061	0.889	0.722	−0.028	0.533	0.474
		$\widehat{\theta}$	−0.139	0.402	0.253	−0.082	0.288	0.201	−0.010	0.199	0.154	−0.005	0.122	0.108
	1	$\widehat{\lambda}$	−0.117	2.418	1.918	−0.048	1.802	1.787	−0.051	1.042	1.337	−0.014	0.419	0.527
		$\widehat{\theta}$	−0.076	1.037	0.800	−0.037	0.771	0.723	−0.028	0.479	0.547	−0.006	0.227	0.246
	2	$\widehat{\lambda}$	−0.262	1.830	0.925	−0.244	1.480	0.877	−0.158	1.437	0.983	−0.151	1.059	0.923
		$\widehat{\theta}$	−0.336	2.183	1.154	−0.332	1.742	1.042	−0.203	1.654	1.089	−0.184	1.231	1.044
2	0.25	$\widehat{\lambda}$	−1.186	3.739	2.198	−0.677	2.646	1.822	−0.225	1.790	1.464	−0.102	1.070	0.981
		$\widehat{\theta}$	−0.153	0.399	0.217	−0.089	0.288	0.184	−0.020	0.201	0.154	−0.011	0.123	0.111
	1	$\widehat{\lambda}$	−0.428	2.748	2.047	−0.212	2.161	1.713	−0.142	1.310	1.226	−0.059	0.769	0.740
		$\widehat{\theta}$	−0.140	0.735	0.593	−0.073	0.547	0.440	−0.054	0.352	0.321	−0.025	0.215	0.202
	2	$\widehat{\lambda}$	−0.714	3.089	1.727	−0.522	2.891	1.719	−0.452	2.579	1.704	−0.259	2.123	1.738
		$\widehat{\theta}$	−0.457	1.825	1.047	−0.340	1.697	1.026	−0.299	1.509	0.994	−0.169	1.223	0.980

Overall, the results indicate that the estimation procedure performs satisfactorily, as both the empirical bias and the RMSE tend to decrease with increasing sample size. A notable aspect of the results is the differing behavior exhibited by the estimators of λ and θ. In general, the shape parameter θ is estimated more accurately than the scale parameter λ, particularly when θ takes small values. For instance, when $(\lambda, \theta) = (2, 0.25)$, the bias of $\widehat{\theta}$ decreases from -0.153 for $n = 50$ to -0.011 for $n = 500$, while the corresponding RMSE decreases from 0.217 to 0.111. In contrast, the estimator of λ exhibits substantially larger variability under the same configuration.

The results also reveal that the estimation problem becomes more challenging when θ takes large values. For configurations with $\theta = 2$, both the bias and the RMSE decrease more slowly as the sample size increases. This effect is particularly noticeable in the estimation of λ, whose RMSE remains relatively large even for $n = 500$. An important point is that this behavior should not be attributed solely to the non-existence of moments. Indeed, Proposition 5 establishes that the SMAK distribution does not possess positive moments for any $\theta > 0$. Therefore, the absence of moments is a general property of the distribution and cannot, by itself, explain why the finite-sample performance is more challenging when $\theta = 2$.

A more plausible explanation is related to the information available for distinguishing the scale and shape parameters in this region of the parameter space. In particular, the likelihood surface may exhibit weaker curvature in some parameter directions, resulting in greater sampling variability and slower stabilization of the maximum likelihood estimators. This interpretation is consistent with the relatively large RMSE observed for $\widehat{\lambda}$ when $\theta = 2$, which remains substantial even for $n = 500$. Thus, the simulation results suggest that the slower reduction in bias observed for $\theta = 2$ is more closely associated with the finite-sample identifiability of the parameters and the local geometry of the likelihood than with the absence of moments, which is common to all parameter configurations considered.

In addition to the estimation accuracy, we assessed the numerical performance of the EM algorithm by recording the number of iterations required for convergence and the computational time in each simulation run. In all simulations, the algorithm was initialized at $(\lambda^{(0)}, \theta^{(0)}) = (1, 1)$, a common and simple starting configuration, and it converged in all 1000 replications for each of the 36 simulation scenarios considered. Across the 36,000 simulation runs, the average number of iterations required for convergence was 1113.6, with scenario-specific averages ranging from 367.9 to 2030.1 iterations; the average computational time was 0.13 s, with scenario-specific averages ranging from 0.05 to 0.28 s.

Despite differences in estimation accuracy across parameter configurations, the overall results indicate that the proposed EM algorithm converges reliably and provides increasingly accurate parameter estimates as sample size grows. These findings support the practical applicability of the proposed estimation procedure for moderate to large sample sizes.

4. Applications with Real Data

This dataset comes from the Survey of Consumer Finances (SCF), a nationally representative sample that contains extensive information on assets, liabilities, income, and demographic characteristics of the respondents (potential U.S. customers). It consists of a random sample of 500 households with positive incomes that were interviewed in the 2004 survey. The data can be accessed from the Federal Reserve's website: https://www.federalreserve.gov/econres/scfindex.htm (accessed on 12 June 2026).

4.1. Income per Capita

In this subsection, the variable of interest is the annual family income, expressed in thousands of U.S. dollars and divided by the number of household members. Table 3 presents the descriptive statistics for these data. Throughout the paper, CS and CK denote the sample skewness and kurtosis coefficients, respectively.

Table 3. Descriptive statistics for income data.

n	Median	Mean	Variance	CS	CK
500	21.125	216.709	1,127,000	12.176	494.470

Figure 3 shows the boxplot of the income per capita data and reveals an extreme observation, suggesting a pronounced right tail. The median income per capita is 21.125 thousand U.S. dollars, whereas the data contain a highly atypical observation corresponding to an income of 75 million U.S. dollars. As shown in Table 3, the sample kurtosis coefficient is extremely high, suggesting that a suitable model should be able to accommodate a pronounced right tail and extreme observations.

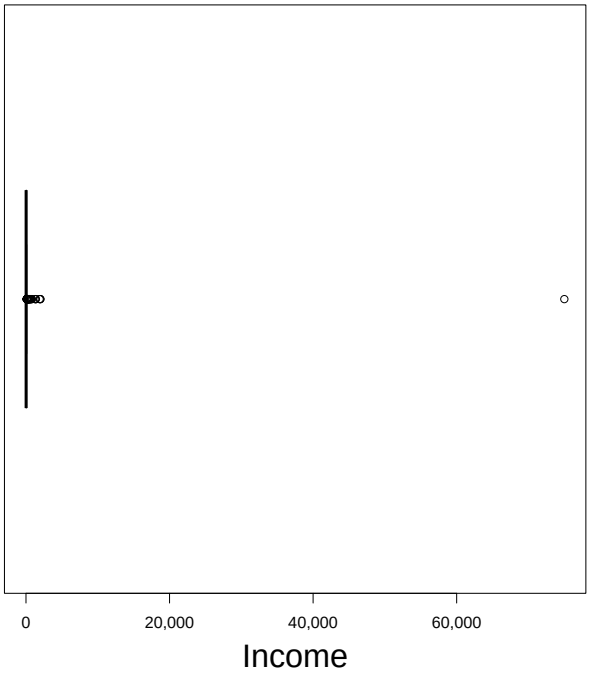


Figure 3. Boxplot for income per capita data.

In the comparative application, we use the AK model to assess the performance of the proposed model in the presence of extreme observations, as well as the lognormal (LN) model, which is widely used for modeling income data. Table 4 presents the ML estimates of the parameters of the SMAK, LN, and AK models, together with their corresponding standard errors and the Akaike Information Criterion (AIC) (see Akaike [23]), the Bayesian Information Criterion (BIC) (see Schwarz [24]), the Kolmogorov–Smirnov (KS), the Anderson–Darling (AD), and the Cramer–Von-Mises (CvM) goodness-of-fit statistics. The SMAK model yields the smallest AIC, BIC, KS, AD, and CvM values among the three competing models, providing consistent evidence of a favorable fit to the data. Figure 4 displays the QQ-plots for the SMAK and LN models. The R codes for this application, together with the dataset, are included as Supplementary Material.

Table 4. ML estimates for the income per capita data, with corresponding standard errors (in parentheses), together with AIC, BIC, KS, AD, and CvM goodness-of-fit statistics.

	SMAK	**LN**	**AK**
λ	2.823 (0.740)	—	—
θ	0.457 (0.097)	—	23.989 (1.697)
μ	—	3.101 (0.064)	—
σ	—	1.432 (0.045)	5166.481 (289.360)
AIC	4840.102	4881.953	6373.741
BIC	4848.531	4890.382	6382.170
KS	0.058	0.067	0.570
AD	1.112	3.639	17.469
CvM	0.176	0.574	2.920

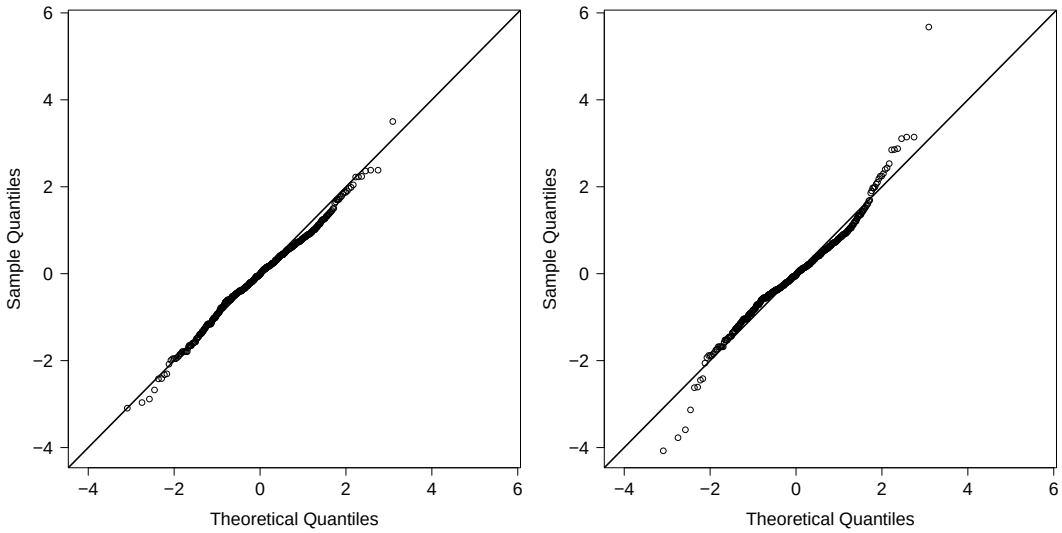


Figure 4. QQ-plots of the SMAK model (**left**) and the lognormal model (**right**) for the income per capita data.

4.2. Income per Family

The variable of interest is the annual family income in thousands of U.S. dollars. Descriptive statistics for these data are presented in Table 5.

Table 5. Descriptive statistics for income per family data.

n	**Median**	**Mean**	**Variance**	**CS**	**CK**
500	54	321.022	11,634,483	21.127	461.575

Figure 5 displays the boxplot of the income data and reveals an extreme observation corresponding to a single-person household. Other atypical observations are also present, suggesting a pronounced right tail. The median income is 54 thousand U.S. dollars per family, while the data contain several very high income values and one extremely high observation of 75 million U.S. dollars. As shown in Table 5, the sample kurtosis coefficient is extremely high, suggesting that a suitable model should be able to accommodate a pronounced right tail and extreme observations. We therefore compare the fit of the SMAK distribution with those of the AK and LN distributions. Table 6 presents the ML estimates of the model parameters, together with their corresponding standard errors and the AIC, BIC, KS, AD, and CvM goodness-of-fit statistics. The SMAK model yields the smallest AIC, BIC, AD, and CvM values, whereas the LN model provides a slightly smaller KS statistic. Overall, these results provide favorable evidence for the SMAK model relative to the competing distributions. Figure 6 shows the QQ-plots of the SMAK and

LN models. The R codes for this application, together with the dataset, are included as Supplementary Material.

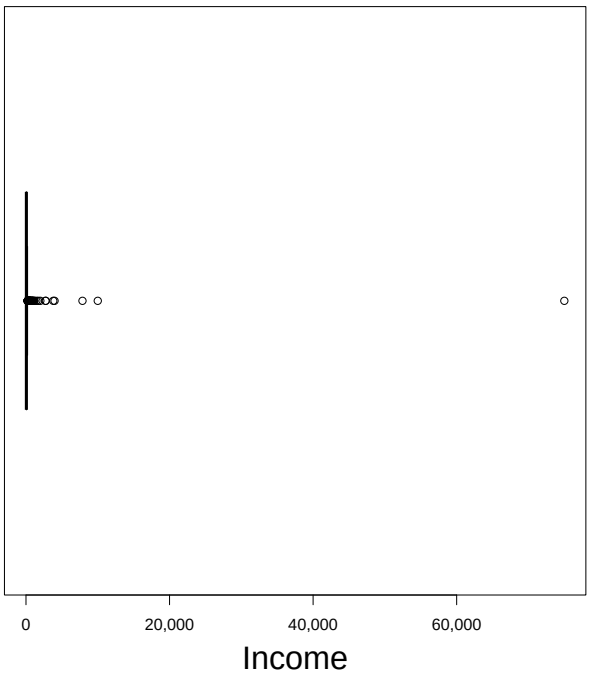


Figure 5. Boxplot for income per family data.

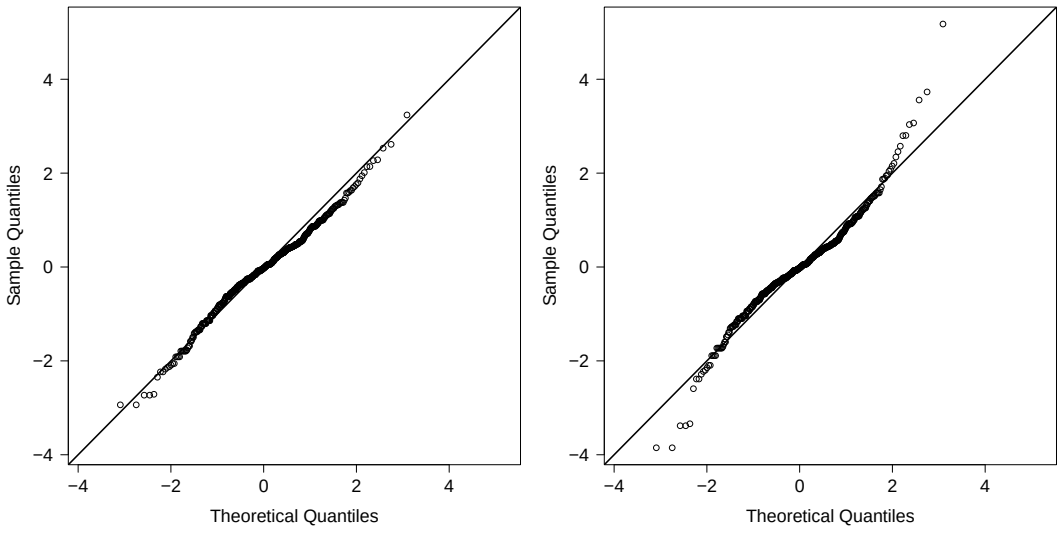


Figure 6. QQ-plots of the SMAK model (**left**) and the lognormal model (**right**) for the income per family data.

Table 6. ML estimates for the income per family data, with corresponding standard errors (in parentheses), together with AIC, BIC, KS, AD, and CvM goodness-of-fit statistics.

	SMAK	**LN**	**AK**
λ	7.758 (1.867)	—	—
θ	0.482 (0.092)	—	13.512 (3.971)
μ	—	4.016 (0.062)	—
σ	—	1.393 (0.044)	4250.416 (1288.685)
AIC	5731.502	5771.058	6761.916
BIC	5739.932	5779.487	6770.345
KS	0.086	0.082	0.478
AD	1.999	5.081	20.711
CvM	0.354	0.887	3.663

4.3. Survival Time (In Days)

The third dataset consists of survival times, measured in days, for 137 patients with advanced lung cancer. These data were obtained from a study conducted by the U.S. Department of Veterans Affairs and were reported by Kalbfleisch and Prentice [25]. The dataset is available in the R package "survival" (see Therneau [26]) under the name "veteran". Table 7 presents the descriptive statistics for these data.

We compare the proposed model with the slash Fréchet (SFr) model (see Castillo et al. [27]) and the slash Lomax–Rayleigh (SLR) model (see Santoro et al. [28]), both of which are flexible distributions capable of accommodating heavy-tailed behavior.

1. The density function of the slash Fréchet (SFr) model is given by

$$f(z;\lambda,\theta) = \frac{\theta}{z^{\theta+1}}\Gamma\left(1-\frac{\theta}{\lambda}, z^{-\lambda}\right), \quad z,\lambda,\theta > 0,$$

where $\lambda > \theta$ and $\Gamma(a,t) = \int_t^{\infty} w^{a-1}e^{-w}dw$ is the incomplete gamma function.

2. The density function of the slash Lomax–Rayleigh (SLR) model is given by

$$f_Z(z;\lambda,\theta) = \theta^2\lambda^{\frac{\theta}{2}}z^{-(\theta+1)}B\left(\frac{z^2}{\lambda+z^2};\frac{\theta}{2}+1,\frac{\theta}{2}\right),$$

where $\lambda > 0$, $\theta > 0$, $z > 0$ and $B(w;a,b) = \int_0^w u^{a-1}(1-u)^{b-1}du$ is the incomplete beta function.

Table 7. Descriptive statistics of survival time (in days) of patients with lung cancer.

n	Mean	Variance	CS	CK
137	121.628	24,906.12	3.092	15.554

Figure 7 displays the boxplot of survival times and reveals an extreme observation. Other atypical observations are also present, suggesting a pronounced right tail. Most patients have survival times of around 80 days, whereas one patient exhibits a remarkably long survival time of 999 days.

Table 8 shows the ML estimates for the third model and their SEs (standard errors), as well as the AIC and BIC criteria. The R codes for this application are provided as Supplementary Material.

Overall, the SMAK distribution provides a better fit to the survival time data than the competing models.

Table 8. ML estimates for the survival time (in days) of patients with lung cancer data, with corresponding standard errors (in parentheses), together with AIC, BIC, KS, AD, and CvM goodness-of-fit statistics.

	SMAK	SFr	SLR
λ	11.517 (5.865)	0.772 (0.198)	630.939 (288.829)
θ	0.610 (0.225)	0.339 (0.085)	1.029 (0.134)
AIC	1600.196	1748.946	1609.428
BIC	1606.036	1754.785	1615.268
KS	0.077	0.327	0.121
AD	1.251	2.395	2.079
CvM	0.230	0.393	0.372

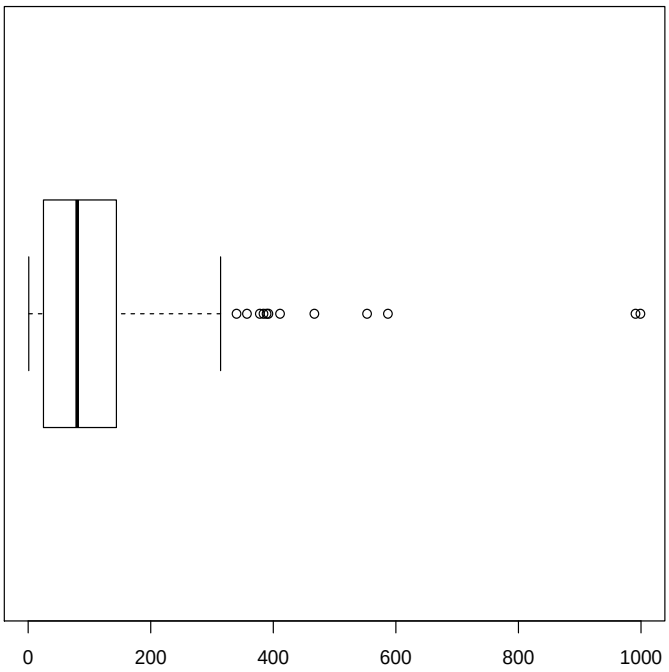


Figure 7. Boxplot for measures of survival time (in days) of patients with lung cancer data.

Figure 8 shows the QQ-plots for the SMAK and SLR models. The QQ-plot for the SMAK model shows a closer agreement between the theoretical and empirical quantiles, particularly in the upper tail, whereas the SLR model exhibits larger deviations from the reference line. This graphical evidence is consistent with the goodness-of-fit measures reported in Table 8, which indicate a favorable fit of the SMAK model to the survival time data.

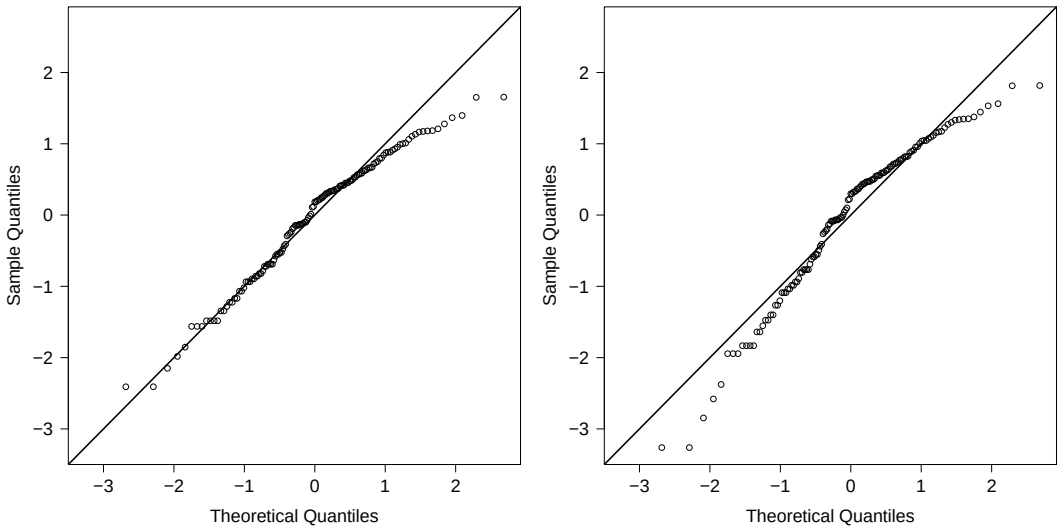


Figure 8. QQ-plots of the SMAK model (**left**) and the SLR model (**right**), for the survival time (in days) of patients with lung cancer data.

5. Conclusions

In this paper, we introduce an extension of the AK distribution using the scale mixture methodology. We study some properties, estimate parameters via the ML method using the EM algorithm, and apply the model to income data. The SMAK distribution results from a scale mixture of the AK and Exponential distributions, yielding a new distribution with a heavy right tail that makes it interesting for use in actuarial statistics and other areas. Some additional features of the SMAK model are as follows:

- The SMAK distribution has a heavy right tail.
- The SMAK distribution has two representations given in Propositions 1 and 2.
- PDF, CDF, and hazard function are explicit.
- The hazard function is decreasing when the shape parameter is less than one, which suggests information regarding the tail of the distribution; that is, a heavy right tail (see Rolski et al. [29]).
- Using the representation given in Proposition 1, it was possible to implement the EM algorithm to compute the ML estimates.
- In the applications, it is shown that the SMAK distribution is a good distribution for modeling data per capita income, family income and survival time (in days) of patients with lung cancer, outperforming a known distributions: the AK, LN, SFr and SLR.
- Since the SMAK distribution has no expectation and variance, future work will study inference based on percentiles.

Supplementary Materials: The following supporting information can be downloaded at https://www.mdpi.com/article/10.3390/axioms15090659/s1, app1.R: R code for Application 1; app2.R: R code for Application 2; app3.R: R code for Application 3; and DATACOMPLETA.txt: Datasets for all applications.

Author Contributions: Conceptualization, N.M.O. and L.F.-L.; methodology, H.W.G.; software, D.I.G. and H.W.G.; validation, N.M.O., O.V., and H.W.G.; formal analysis, N.M.O. and H.W.G.; investigation, L.F.-L. and O.V.; writing—original draft preparation, D.I.G. and N.M.O.; writing—review and editing, L.F.-L. and O.V. All authors have read and agreed to the published version of the manuscript.

Funding: L.F.-L. was supported by DICREA, Universidad del Bio-Bio, Chile.

Institutional Review Board Statement: Not applicable.

Informed Consent Statement: Not applicable.

Data Availability Statement: Data for the first and second applications are available at https://www.federalreserve.gov/econres/scfindex.htm (accessed on 12 June 2026), while those for the third is available in the R package "survival" (see Therneau [26]).

Conflicts of Interest: The authors declare no conflicts of interest.

References

1. Johnson, N.L.; Kotz, S.; Balakrishnan, N. *Continuous Univariate Distributions*, 2nd ed.; Wiley: New York, NY, USA, 1995; Volume 1.
2. Rogers, W.H.; Tukey, J.W. Understanding some long-tailed symmetrical distributions. *Stat. Neerl.* **1972**, *26*, 211–226. [CrossRef]
3. Mosteller, F.; Tukey, J.W. *Data Analysis and Regression*; Addison-Wesley: Reading, MA, USA, 1977.
4. Kafadar, K. A biweight approach to the one-sample problem. *J. Amer. Stat. Assoc.* **1982**, *77*, 416–424. [CrossRef]
5. Wang, J.; Genton, M.G. The multivariate skew-slash distribution. *J. Stat. Plan. Inference* **2006**, *136*, 209–220. [CrossRef]
6. Gómez, H.W.; Quintana, F.A.; Torres, F.J. A New Family of Slash-Distributions with Elliptical Contours. *Stat. Probab. Lett.* **2007**, *77*, 717–725. Erratum in *Stat. Probab. Lett.* **2008**, *78*, 2273–2274. [CrossRef]
7. Olmos, N.M.; Varela, H.; Bolfarine, H.; Gómez, H.W. An extension of the generalized half-normal distribution. *Stat. Pap.* **2014**, *55*, 967–981. [CrossRef]
8. Astorga, J.M.; Reyes, J.; Santoro, K.I.; Venegas, O.; Gómez, H.W. A Reliability Model Based on the Incomplete Generalized Integro-Exponential Function. *Mathematics* **2020**, *8*, 1537. [CrossRef]
9. Gómez, Y.M.; Firinguetti-Limone, L.; Gallardo, D.I.; Gómez, H.W. An Extension of the Akash Distribution: Properties, Inference and Application. *Mathematics* **2024**, *12*, 31. [CrossRef]
10. Andrews, D.F.; Mallows, C.L. Scale mixtures of normal distributions. *J. R. Stat. Soc. Ser. B* **1974**, *36*, 99–102. [CrossRef]
11. Shanker, R. Akash Distribution and Its Applications. *Int. J. Probab. Stat.* **2015**, *4*, 65–75.
12. Shanker, R.; Shukla, K.K. On Two-Parameter Akash Distribution. *Biom. Biostat. Int. J.* **2017**, *6*, 00178. [CrossRef]
13. Shanker, R.; Shukla, K.K. Power Akash Distribution and Its Application. *J. Appl. Quant. Methods* **2017**, *12*, 1–10. [CrossRef]

14. Foss, S.; Korshunov, D.; Zachary, S. *An Introduction to Heavy-Tailed and Subexponential Distributions*, 2nd ed.; Springer Series in Operations Research and Financial Engineering; Springer: Berlin/Heidelberg, Germany, 2013.
15. Aitchison, J.; Brown, J.A.C. *The Lognormal Distribution*; Cambridge University Press: Cambridge, UK, 1957.
16. Kleiber, C.; Kotz, S. *Statistical Size Distributions in Economics and Actuarial Sciences*; John Wiley: Hoboken, NJ, USA, 2003.
17. Tanner, M.A. *Tools for Statistical Inference*, 3rd ed.; Springer: New York, NY, USA, 1996. [CrossRef]
18. Beirlant, J.; Matthys, G.; Dierckx, G. Heavy-tailed distributions and rating. *ASTIN Bull.* **2001**, *31*, 37–58. [CrossRef]
19. Zhao, J.; Ahmad, Z.; Mahmoudi, E.; Hafez, E.H.; El-Din, M.M.M. A New Class of Heavy-Tailed Distributions: Modeling and Simulating Actuarial Measures. *Complexity* **2021**, 2021, 5580228. [CrossRef]
20. Riad, F.H.; Radwan, A.; Almetwally, E.M.; Elgarhy, M. A new heavy tailed distribution with actuarial measures. *J. Radiat. Res. Appl. Sci.* **2023**, *16*, 100562. [CrossRef]
21. Afify, A.Z.; Pescim, R.R.; Cordeiro, G.M.; Mahran, H.A. A New Heavy-Tailed Exponential Distribution: Inference, Regression Model and Applications. *Pak. J. Stat. Oper. Res.* **2023**, *19*, 395–411. [CrossRef]
22. Dempster, A.P.; Laird, N.M.; Rubin, D.B. Maximum likelihood from incomplete data via the EM algorithm (with discussion). *J. R. Stat. Soc. B Stat. Methodol.* **1977**, *39*, 1–38. [CrossRef]
23. Akaike, H. A new look at the statistical model identification. *IEEE Trans. Autom. Control* **1974**, *19*, 716–723. [CrossRef]
24. Schwarz, G. Estimating the dimension of a model. *Ann. Stat.* **1978**, *6*, 461–464. [CrossRef]
25. Kalbfleisch, J.D.; Prentice, R.L. *The Statistical Analysis of Failure Time Data*; John Wiley & Sons: New York, NY, USA, 1980.
26. Therneau, T. *A Package for Survival Analysis in R*, R package version 3.5-7; 2023. Available online: https://CRAN.R-project.org/package=survival (accessed on 12 March 2023).
27. Castillo, J.S.; Rojas, M.A.; Reyes, J. A More Flexible Extension of the Fréchet Distribution Based on the Incomplete Gamma Function and Applications. *Symmetry* **2023**, *15*, 1608. [CrossRef]
28. Santoro, K.I.; Gallardo, D.I.; Venegas, O.; Cortés, I.E.; Gómez, H.W. A Heavy-Tailed Distribution Based on the Lomax–Rayleigh Distribution with Applications to Medical Data. *Mathematics* **2023**, *11*, 4626. [CrossRef]
29. Rolski, T.; Schmidli, H.; Schmidt, V.; Teugel, J. *Stochastic Processes for Insurance and Finance*; John Wiley & Sons: New York, NY, USA, 1999.

Disclaimer/Publisher's Note: The statements, opinions and data contained in all publications are solely those of the individual author(s) and contributor(s) and not of MDPI and/or the editor(s). MDPI and/or the editor(s) disclaim responsibility for any injury to people or property resulting from any ideas, methods, instructions or products referred to in the content.